

**Erf affects commitment and differentiation of osteoprogenitor cells in cranial sutures via the retinoic acid pathway**

Angeliki Vogiatzi<sup>1</sup>, Ismini Baltsavia<sup>1</sup>, Emmanuel Dialynas<sup>2</sup>, Vassiliki Theodorou<sup>2</sup>, Yan Zhou<sup>3</sup>, Elena Deligianni<sup>2</sup>, Ioannis Iliopoulos<sup>1</sup>, Andrew O. M. Wilkie<sup>3</sup>, Stephen R. F. Twigg<sup>3</sup>, and George Mavrothalassitis<sup>1,2,\*</sup>

*Short title: Erf in craniosynostosis*

<sup>1</sup> Medical School, University of Crete, Heraklion, Crete, 71003, Greece

<sup>2</sup> IMBB, FORTH, Heraklion, Crete, 70013, Greece

<sup>3</sup> MRC Weatherall Institute of Molecular Medicine, University of Oxford, Oxford, OX3 9DS, UK

\* corresponding author. Email: [mavro@imbb.forth.gr](mailto:mavro@imbb.forth.gr), Tel: +30-2810-394537, Fax +30-2810-394530

## Abstract

ETS2 repressor factor (ERF) haploinsufficiency causes late onset craniosynostosis (OMIM 600775; CRS4) in humans while in mice Erf-insufficiency also leads to a similar multi-suture synostosis phenotype preceded by mildly reduced calvarium ossification. However, neither the cell types affected nor the effects per se have been identified so far. Here we establish an *ex vivo* system for the expansion of suture-derived mesenchymal stem and progenitor cells (sdMSCs) and analyze the role of Erf levels in their differentiation. Cellular data suggest that Erf-insufficiency specifically decreases osteogenic differentiation of sdMSCs resulting in the initially delayed mineralization of the calvarium. Transcriptome analysis indicates that Erf is required for efficient osteogenic lineage commitment of sdMSCs. Elevated retinoic acid catabolism due to increased levels of the cytochrome P450 superfamily member *Cyp26b1* as a result of decreased Erf levels appears to be the underlying mechanism leading to defective differentiation. Exogenous addition of retinoic acid can rescue the osteogenic differentiation defect suggesting that Erf affects cranial bone mineralization during skull development through retinoic acid gradient regulation

## Introduction

Cranial sutures comprise the connective tissues between the bones of the skull and are considered to be major centres of bone growth during development (1, 2). Mesenchymal stem cells that reside in the suture mesenchyme, commit and enter the intramembranous ossification pathway giving rise to proliferating populations of osteoprogenitor and preosteoblast cells that eventually differentiate to osteoblasts at the edges of the developing bones (3, 4). The balance between the different cell types seems to be crucial for suture patency and consequently for the coordination of skull and brain development (5, 6). Craniosynostosis is a developmental disorder in which one or more of the cranial sutures close prematurely, leading to skull and facial deformities along with complications that can affect vision, hearing, breathing and learning ability. During the last 25 years, considerable effort has been put into unraveling the mechanisms that underlie craniosynostosis (7). However, the presence of multiple cell populations in sutures, the paucity of specific cellular markers and difficulties in the identification and isolation of suture stem cells, have hindered these efforts.

Genetic analysis has identified an increasing number of genes that, when mutated, cause craniosynostosis. Activating mutations in three members of the fibroblast growth factor receptor family (FGFR1, FGFR2, FGFR3) and alterations in downstream signalling cascades such as the p38 MAPK, ERK1/2, PI3K/AKT and PLC $\gamma$ /PKC pathways have been commonly reported to be involved in syndromic cases (8-14). We previously reported that haploinsufficiency of the ets-domain transcriptional repressor factor ERF, a downstream target of ERKs that can regulate cellular proliferation and differentiation (15-18), causes premature suture closure in humans (19, 20). This disorder, termed ERF-related craniosynostosis (CRS4; OMIM 61188) ranges widely in severity. Children affected by this disorder present synostosis after infancy more frequently compared to other craniosynostosis cases and sometimes this is associated with an insidious onset of raised intracranial pressure causing permanent visual impairment (19, 20). Although mice with the equivalent genotype (*Erf*<sup>+/-</sup>) are phenotypically normal, by reducing the *Erf* dosage further to ~30% of wild-type by combining loss-of-function (*Erf*) and hypomorphic

(*Erf*<sup>doxP</sup>) alleles in *trans*, the resulting *Erf*-insufficient mice (*Erf*<sup>doxP/-</sup> mice) display facial dysmorphism with no other obvious skeletal defects beyond craniosynostosis and a mild reduction in the ossification of calvarial bones, closely recapitulating the human disease (20).

Retinoic acid (RA) acting as a morphogen regulates developmental processes through concentration gradients in multiple systems. Neural crest cell induction, pharyngeal arch and trunk formation, heart, eye and limb development are among the biological events shown to be dependent on RA signalling (21-28). Calvarial bone formation seems to be also sensitive to retinoic acid concentration and action. Excessive amounts of RA have been shown to have teratogenic effects during pregnancy causing multiple craniofacial abnormalities to embryos (29-31). Hypomorphic and null mutations in the gene coding for *CYP26B1*, the RA-catabolizing enzyme, lead to cranial bone hypoplasia and craniosynostosis in humans (32), while significant decrease in *Retinol-binding protein 4 (RBP4)*, necessary for retinol transport, is detected in sutures from children with craniosynostosis in an independent study (33). In zebrafish, *cyp26b1* is shown to be expressed at the osteogenic fronts after suture formation and its partial loss results in craniosynostosis (32). Interestingly, *Cyp26b1*(-/-) mice display multiple abnormalities in facial structures along with reduced ossification of the calvarial bones at E18.5 but not craniosynostosis (34). At the cellular level, the commitment of cranial bone mesenchymal progenitor cells along the osteogenic lineage in mice has been shown to be sensitive to balanced levels of retinoic acid and the epigenetic methyltransferase *Ezh2* (35, 36). The diversity of the RA-associated phenotypes indicate that the precise retinoic acid spatiotemporal regulation is crucial for normal cranial bone and suture formation. Surprisingly, there is limited information on the factors that regulate RA signalling during calvarial development.

In the present study by introducing modifications into previous suture cell isolation methods (37, 38), we developed a new approach to derive mesenchymal stem/ progenitor cells from cranial sutures of *Erf*-competent (*Erf*<sup>doxP/+</sup>) and *Erf*-insufficient (*Erf*<sup>doxP/-</sup>) mice to evaluate their function. *Ex vivo* cellular differentiation studies of these suture-derived mesenchymal stem/ progenitor cells (sdMSCs), show that decreased levels of *Erf* result in decreased osteogenic commitment and

differentiation. Transcriptome analysis and correlation studies corroborate the cellular data and suggest that reduced retinoic acid signalling due to increased levels of the RA-catabolizing factor *Cyp26b1* may underlie the phenotype of Erf-insufficient cells. Exogenous addition of retinoic acid during sdMSC *in vitro* differentiation fully suppresses the osteogenic differentiation defect of Erf-insufficient cells without affecting the Erf-competent cell cultures. Our data indicate that Erf may affect cranial suture development via retinoic acid regulation, providing a link in the FGF-RA control loop (39, 40).

## **Results**

### *LIF-selected long-term expanded suture derived cells possess in vitro characteristics of mesenchymal stem/progenitor cells*

Cranial sutures constitute niches of highly heterogeneous cell populations related to bone growth (37). We thus focused our efforts on mesenchymal stem cell (MSC) derived populations and based on previous studies we established a new protocol utilizing leukemia inhibitory factor (LIF) for the selective expansion and maintenance of mesenchymal stem/progenitor cells from cranial sutures. Suture explants from postnatal day 5 (P5) mice and resulting suture-derived cells were cultured in the presence of leukemia inhibitory factor (LIF), known for its role in sustaining the stem cell state while inhibiting differentiation (41, 42). Cultivation of suture-derived cells in the presence of LIF for a minimum of 8 population doublings (PDs) during a period of 50-60 days resulted in a population of cells that were plastic-adherent, fibroblast-like in shape (Figure 1A, B) and expressed increased levels of the MSC marker *Axin2* (43), and reduced levels of the osteogenic differentiation marker *Sp7*, compared to the initial population (Figure 1C). The majority of these cells expressed the MSCs-associated surface antigens CD44, CD90, CD29 and Sca1 (4, 44-46), while neither hematopoietic nor endothelial cell markers could be detected (Figure 1D). This cell population growing in culture for more than 8 PDs could effectively undergo differentiation towards the chondrogenic, osteogenic and adipogenic lineages (Figure 1E), a hallmark of mesenchymal stem

cells. These cells, which we label suture-derived mesenchymal stem/ progenitor cells (sdMSCs), can be routinely maintained in culture for more than 20 PDs (Figure 1F) and sustain their characteristics for at least 3 freeze-thaw cycles.

Utilizing this approach we established sdMSCs from  $Erf^{loxP/+}$  and  $Erf^{loxP/-}$  P5 littermates, in at least 5 independent experiments, to study the effect of limited Erf levels on MSC growth and differentiation. At this time-point the mice have not yet developed the phenotype of synostosis.

### *Erf insufficiency compromises the commitment of suture mesenchymal stem/ progenitor cells towards the osteogenic lineage*

Although Erf is known to affect cellular proliferation (16, 47), cell cycle phase analysis of  $Erf^{loxP/+}$  and  $Erf^{loxP/-}$  sdMSCs showed no significant difference in the cell distribution profiles (Figure 2A). There was also no difference in the cell doubling time throughout the life of the cultures (Figure 2B), suggesting that Erf insufficiency does not affect sdMSC self-renewal rate. We then examined the impact of Erf levels on sdMSC differentiation.  $Erf^{loxP/+}$  and  $Erf^{loxP/-}$  cells showed comparable efficiency in *in vitro* chondrogenic and adipogenic commitment (Figure 2C and D). However,  $Erf^{loxP/-}$  cells displayed decreased ability to mineralize (Figure 2E and F), implying an impairment in the osteogenic differentiation of these cells. The reduced osteogenic differentiation was also apparent in the initial heterogeneous suture-derived cell population where  $Erf^{loxP/-}$  cells displayed initially comparable but later decreased capacity to mineralize (Figure 3A, B). Chondrogenic differentiation appeared unaffected, while the limited adipogenic differentiation was increased in  $Erf^{loxP/-}$  cells (Figure 3C-E), indicating possibly the existence of a greater proportion of precursor populations among Erf-insufficient suture cells. These results indicate that the insufficiency of Erf reduces the osteogenic ability of suture-derived cells *in vitro*.

To gain further insight into the apparent differences in sdMSC osteogenic differentiation and understand the possible role of Erf levels in this process, we analyzed transcriptome changes in suture derived cells from  $Erf^{loxP/+}$  and  $Erf^{loxP/-}$  mice in 3 conditions. sdMSCs at PD8 in self-renewal or osteogenic differentiation medium for 24h were used for early differentiation events, while the initial

heterogeneous suture cell population growing in expansion media without LIF was used as a mixed differentiation state specimen (Figure 4A). Consistent with the decrease rather than elimination of *Erf* expression, a very limited number of genes were found to differ between the two genotypes. This was evident by the clustering of transcriptome samples according to culture conditions but not genotypes (Figure 4B and Table 1). However, all 3 growth conditions produced distinct patterns that clustered together assuring the consistency of the *ex vivo* cultures (Figure 4C). The limited number of differentially expressed genes indicated a deficit of core matrisome genes in *Erf*<sup>loxP/-</sup> cells when tested against the GSEA database (48) (Figure 5A and B and Table 1) supporting that *Erf* insufficiency leads to a defect in the osteogenic differentiation. This was consistent with the transcriptome differences of *Erf*-competent and *Erf*-insufficient cells upon osteogenic induction (Supplementary Table 1). *Erf*<sup>loxP/-</sup> cells exhibited considerably fewer genes associated with ossification and extracellular matrix organization than *Erf*<sup>loxP/+</sup> cells during induction of sdMSCs (Figure 5C, L-O minus and L-O plus). Consistently, *Erf*<sup>loxP/-</sup> sdMSCs either self-renewing or differentiating for 24h required many more ossification-related changes to reach the differentiation state of the initial heterogeneous cell population than the *Erf*<sup>loxP/+</sup> cells (Figure 5C, O-F minus and O-F plus).

We further examined the apparent contribution of *Erf* expression in the effective osteogenic differentiation, interrogating single cell RNA-sequencing data from mouse sutures available through the facebase consortium (49, 50). Given the ubiquitous expression of *Erf* and its post transcriptional regulation we developed an approach to examine gene co-expression rather than cell cluster expression. We determined any expression correlation between the gene of interest and the rest of the cellular transcripts for each informative cell in the data, and evaluated the known function of the correlated genes. *Erf* expression appeared to correlate with genes involved in ossification and extracellular matrix organization (Figure 6A and Supplementary Table 2). When compared to other suture ossification landmark genes subjected to the same correlation analysis, *Erf* clustered closely to *Sp7* in cells at E16.5 and *Fgfr1*, *Runx2*, *Twist1* and *Alpl* in cells at E18.5 and P10 (Figure 6B and Supplementary Table 2).

These data suggest that appropriate *Erf* expression level is required for proper differentiation of cranial suture cells towards the osteogenic pathway and are consistent with the decreased mineralization pattern observed previously *in vivo* (20), that could account for the late-onset of *Erf*-related synostosis phenotype.

#### *Erf-insufficiency-induced osteogenic defect can be rescued by retinoic acid*

In spite of the limited number of genes found to differ between *Erf*-competent and *Erf*-insufficient cells in all growth conditions, a group of genes associated with the retinoic acid (RA) pathway could be identified (Table 1). Characteristically, *Cyp26b1*, a gene coding for a RA-catabolizing enzyme known to affect suture development leading to craniosynostosis (32), was elevated upon *Erf* insufficiency in both proliferating and differentiating sdMSCs and in the initial heterogeneous suture cell population (Table 1 and Figure 7A). *Cyp26b1* was drastically reduced upon normal sdMSC differentiation but remained in relatively high levels in *Erf*-insufficient cells (Figure 7B) suggesting decreased levels of retinoic acid. Comparison of the genes differentially expressed during the differentiation of *Erf*-competent and *Erf*-insufficient sdMSCs, with genes regulated by retinoic acid in mouse embryonic stem cells (ESCs) (51, 52) reveals a 4 to 5 orders of magnitude higher significance for the *Erf*-competent (*Erf*<sup>doxP/+</sup>) cell gene set (Figure 7C, and Supplementary Tables 3 and 4). Analysis of these common genes (Supplementary Table 4) through metascape (53) indicated that indeed in the case of *Erf*-competent (*Erf*<sup>doxP/+</sup>) cells, they are associated with genes known to play a major role in suture development as *Runx*, *Twist* and *BMP-Smad*. In contrast, in the case of *Erf*-insufficient (*Erf*<sup>doxP/-</sup>) cells, they appear to associate with lymphoid and endothelial pathways (Figure 7D). It would thus appear that *Erf*-deficiency leads to a decreased retinoic acid response affecting suture development.

Retinoic acid affects multiple developmental processes and pathways and has been suggested that its homeostasis is crucial for normal skeletogenesis (33, 54, 55). We thus evaluated the effect of RA on *Erf*-competent and *Erf*-insufficient sdMSCs. A characteristic feature of the differentiating suture-related *Erf*<sup>doxP/-</sup> sdMSCs, is the higher initial proliferation and final cell numbers (Figure 7E and F),



consistent with their decreased capacity to exit self-renewal and commit. Addition of retinoic acid at low concentrations does not appear to affect the growth/survival of Erf-competent sdMSCs (Figure 7G). However, RA addition fully suppressed the increased cell numbers of the differentiating Erf-insufficient cells (Figure 7G). More importantly, the decreased mineralization potential of *Erf*<sup>loxP/-</sup> cells was fully alleviated in the presence of RA without affecting the potential of the Erf-competent cells (Figure 7H).

These data strongly suggest that Erf deficiency decreases retinoic acid levels leading to increased cellular proliferation and decreased osteogenic differentiation. Such changes could be the underlying cause of the late onset Erf-related craniosynostosis phenotype.

## Discussion

Syndromic craniosynostosis due to *ERF* haploinsufficiency presents some unique challenges and opportunities for disease understanding and management. In contrast to FGFR/MAPK-driven craniosynostosis syndromes, it has a late onset phenotype, variable severity and, in the mouse model, an initially decreased calvarial ossification. It would thus appear that Erf could mediate effects at multiple stages during suture development.

Understanding the formation of the cranial sutures is a challenging problem hampered by the multiple origins of the involved cells. We thus established a reliable and reproducible system to derive mesenchymal stem cells from murine cranial sutures and address the contribution of Erf levels in the process. Our cellular data indicate that although *Erf* elimination can affect multiple developmental processes, Erf-insufficiency specifically attenuates osteogenic differentiation. This would be consistent with the role of Erk1/2 in sustaining the undifferentiated state of mesenchymal stem cells (56) and conforms with the absence of other major developmental defects in *Erf*<sup>+/-</sup> and *Erf*<sup>loxP/-</sup> mice (17, 18, 20). The transcriptional changes directly associated with Erf-insufficiency were fairly limited, probably because the 50% reduction in *Erf* may not be sufficient to induce extensive quantitative changes that would evade our detection cutoff limits. However, the

expression program during the differentiation of the sdMSCs was altered extensively as a result of the decreased Erf levels, suggesting a homeostatic effect or an effect on one or more morphogenetic factors.

One consistent effect of Erf-insufficiency through all biological replicates and culture conditions was the elevated expression of *Cyp26b1*, a major retinoic acid catabolizing enzyme, suggesting a possible decrease in retinoic acid levels thus affecting bone development (32-35, 54, 55, 57, 58). Consistently, addition of RA during differentiation of sdMSCs fully alleviated the Erf-deficiency defect, with no apparent effect to Erf competent cells, suggesting that *Erf* through *Cyp26b1* regulation affects retinoic acid levels thus controlling the differentiation outcome. The inhibitory effect of Erf on *Cyp26b1* and the concomitant increase in retinoic acid levels would be consistent with the role of FGF that has already been reported to activate *Cyp26b1* and downregulate RA availability (39, 40, 59). Given that Erf is inactivated via nuclear export as a result of Fgf signaling, the decreased Erf levels would resemble the increased Fgf signaling state.

It is unclear at this point if Erf regulates *Cyp26b1* directly or indirectly. Chromatin occupancy experiments in four independent mouse and human cellular systems, from our laboratory and others (20, 60-62), fail to identify any ERF binding site in the vicinity of *Cyp26b1*. The closest Erf chromatin binding site appears to be 300-400kb away in the proximity of the *Exoc6b* gene rather than *Cyp26b1*. Neither reports of other ets-domain transcription factors directly affecting *Cyp26b1* transcription, nor any confirmed functional ets-binding motifs in its regulatory regions have been found so far. Thus, Erf could affect its expression, either through a distal control element or indirectly by inhibiting a *Cyp26b1* activator (Figure 8).

It is also conceivable that Erf levels affect MSC differentiation and homeostasis in synergy or in competition with other factors. We have previously shown a close proximity of Erf with Runx binding sites and a possible orchestrated regulation by the two factors (20). Erf could antagonize other Ets proteins, such as *Ets1* and *Ets2* that have been reported to affect skull shape and osteogenic differentiation (63, 64). Interestingly, genes differentially affected during Erf-competent and Erf-insufficient cell differentiation harboring sites identified in Erf ChIP-seq experiments, have these sites almost exclusively in putative regulatory

regions and away from the transcription start site where the repressive effect of *Erf* is more prominent (Supplementary Table 5). It would thus appear that *Erf* in an orchestrated manner with other transcription factors, could regulate the homeostasis and kinetics of the process rather than being instructive.

The delayed ossification observed in MSC cultures may directly explain the early ossification defect observed in *Erf*-insufficient mice but may also be responsible of the craniosynostosis phenotype. The decreased MSC differentiation may lead to decreased populations of committed progenitor cells within the suture which in turn fail to keep the suture open, resulting in craniosynostosis. Stem cell depletion (4), osteogenic differentiation-proliferation imbalance (6, 65, 66) and growth dynamics (67) have been previously proposed as potential mechanisms of synostosis. Indeed, there are several systems where *Erf* regulates differentiation. Chorionic trophoblast differentiation depends on *Erf* presence (17), *Erf* blocks the differentiation of Ras-deficient mESCs (62), and the rate of embryonic hematopoietic differentiation depends on *Erf* level (18). Whether *Erf* has additional roles, either positive or inhibitory ones, at later stages of the osteogenic differentiation pathway remains to be explored. Such an inhibitory effect in suture preosteoblast differentiation would be consistent with the reported function of *Erk* in late stages of osteogenic pathway (68-70) as well as the role of *Runx2* in osteogenic differentiation and the antagonistic role of *Erf* (20) that could account for the craniosynostosis phenotype. Interestingly comparable concentrations of retinoic acid have opposite effects on the mineralization of mesenchymal stem cells and more differentiated osteogenic populations such as MC3T3 preosteoblasts, with the former being induced and the latter being suppressed by RA (58, 71-75). Therefore, it is plausible that *Erf*, either through retinoic acid signalling or independently, could also affect the osteogenic pathway at later stages. Upon *Erf* deficiency the initial decreased MSC differentiation and osteoprogenitor expansion could lead to decreased ossification, while an accelerated differentiation of progenitors when they comprise the predominant suture cell population, could lead to depletion and premature ossification of the suture. Further studies would be necessary to explore the spatiotemporal function of *Erf* and its effect on RA concentration gradients in cranial bone and suture development.

In conclusion our work provides evidence that Erf, an effector within the FGF/ERK pathway, affects suture formation and calvarial ossification through the regulation of retinoic acid levels.

## **Materials and Methods**

### *Mouse lines*

Mice were bred and maintained in the animal facility of the Institute of Molecular Biology and Biotechnology in Greece. All experimental protocols were conducted with ethical guidelines and in compliance with the 3Rs. Protocols were approved by the bioethics committee of IMBB and licensed from the General Directorate of Veterinary Services, Region Crete (permit numbers EL 91BIO-02 and EL91-BIOexp-02; project license no. 27289 to G. Mavrothalassitis). *Erf*<sup>loxP/+</sup> and *Erf*<sup>loxP/-</sup> littermates were obtained from crossing *Erf*<sup>+/-</sup> mice with *Erf*<sup>loxP/loxP</sup> mice, both of which have been reported in the literature (20).

### *Suture Cell Cultures and Differentiation Assays*

Freshly isolated cranial suture cells were obtained as described previously (37, 58). Briefly, sagittal and coronal sutures containing approximately 0.5 mm bony margins were dissected from skulls of 5-day-old mice (P5). Following the removal of skin and dura mater, the suture explants were placed into 100mm- cell culture dishes, cut into tiny pieces and cultured in the presence of DMEM-F12 medium (Gibco by Thermo Scientific 31330038) supplemented with 10% fetal bovine serum (Gibco by Thermo Scientific 10270106) and 100 U/ml penicillin/ streptomycin (Gibco by Thermo Scientific 15140122) for 7 days. To obtain suture-derived long-term expanded mesenchymal stem/ progenitor cells, suture explants were cultured into gelatinized dishes in the presence of KnockOut DMEM medium (Gibco by Thermo Scientific 10829018) supplemented with 12% FBS (HyClone GE Healthcare SV30160.03), 2 mM L-glutamine (Gibco by Thermo Scientific 25030024), 1% non-essential amino acids- MEM-NEAA (Gibco by Thermo Scientific 11140050), 100

U/ml penicillin/ streptomycin, 0.1 mM  $\beta$ -mercaptoethanol and 0.3% v/v leukemia inhibitory factor- LIF (produced in our laboratory) for 7 days. Cells were then harvested and further cultured (without the explants) under the same conditions for a total of at least 8 population doublings (PDs) during a period of approximately 50-60 days (Figure 1A). The cumulative population doubling level (CPD) was calculated as described in previous studies (76). At this stage the cells were immunophenotypically evaluated by flow cytometric analysis and checked for osteogenic, chondrogenic and adipogenic differentiation potential.

Osteogenic and chondrogenic differentiation was performed as described previously (77, 78). Osteogenesis was induced in 60-70% confluent cultures by the addition of DMEM- low glucose medium (Gibco by Thermo Scientific 21885025) supplemented with 10% FBS, 0.1  $\mu$ M dexamethasone, 50  $\mu$ M ascorbate-2-phosphate and 10 mM  $\beta$ -glycerophosphate. In the experiments with retinoic acid, freshly prepared osteogenesis medium was supplemented with all-*trans* retinoic acid at a final concentration of 0.5  $\mu$ M before every medium change. Adipogenesis was induced in post-confluent cultures by switching between adipogenic induction and adipogenic maintenance medium (79). One cycle of induction-maintenance was performed for freshly isolated suture cells and 3 cycles for LIF-selection subjected long-term expanded mesenchymal stem/ progenitor cells. To assess the extent of differentiation, staining of cultures with Oil Red O (Sigma O-9755) and Alcian blue (Sigma A-5268) was performed for the detection of adipocytes and cartilage respectively. The evaluation of osteogenic differentiation was performed by Alizarin Red S (Sigma A-5533) staining of the cultures followed by acetic acid extraction and quantification of the dye at 405 nm as already described (80).

#### *Cell growth and viability studies*

Cell doubling time was estimated at specific population doubling levels of the culture by using the already described logarithmic equation (81). The cell cycle phase study was performed in isolated nuclei by propidium iodide (PI) staining of cells in hypotonic solution (82) followed by flow cytometric analysis. Cells of population doubling level 20 (20 PDs) at 60-70% culture confluency were used in all cell cycle experiments. Data were analysed using ModFitLT<sup>TM</sup> software. In order to

evaluate the viability of cells during the osteogenic differentiation, MTT assay was conducted and formazan absorbance was measured at 600 nm (83).

For *in vitro* proliferation assays, bromodeoxyuridine (BrdU) (Sigma B5002) was added to the cell culture medium at a final concentration of 10  $\mu$ M for 8 hours followed by fixation of the cells with 4% paraformaldehyde (PFA) solution. The detection of BrdU positive cells was performed using the following antibodies and reagents: rat anti-BrdU antibody (AbD Serotec MCA2060GA) at a dilution of 1:800, biotin-conjugated anti-rat antibody (Sigma B7139) at 1:100 and FITC-conjugated streptavidin (Biolegend 405201) at 1:1000. A TCS SP2 confocal microscope (Leica microsystems) and an Operetta imaging system were used for signal visualization and analysis.

#### *Flow cytometric analysis*

LIF-selection subjected mesenchymal stem/ progenitor cells of 8 PDs were harvested using 0.25% Trypsin- EDTA solution (Gibco by Thermo Scientific 25200072) for 2 min at 37 °C and stained with the following antibodies in 1% FBS-PBS solution for 30 min at 4 °C: FITC-conjugated anti-CD44 (Biolegend 103006) at a dilution of 1:100, APC-conjugated anti-Sca1 (Biolegend 108111) at 1:100, PE-conjugated anti-CD105 (Biolegend 120407) at 1:200, PE/Cy5-conjugated anti-CD29 (Biolegend 102219) at 1:200, PE/Cy7-conjugated anti-CD90.2 (Biolegend 105325) at 1:600, PerCP/Cy5.5-conjugated anti-CD45 (Biolegend 103131) at 1:400, PE-conjugated anti-CD31 (BD Pharmingen 553373) at 1:200 and APC-conjugated anti-CD34 (Biolegend 119309) at 1:100. A Becton Dickinson FACSCalibur flow cytometer was used in all experiments. The analysis was performed using Flowing Software 2.5.1 version.

#### *Quantitative PCR*

Total RNA was extracted from cultured suture cells using TRI reagent (SIGMA T9424) according to company's instructions. The mRNA was reverse transcribed using SuperScript first-strand synthesis kit (11904-018) and 5 ng of the total synthesized cDNA was added in each real-time qPCR reaction using 2 x Brilliant III SYBR green QPCR master mix (600882-51; Agilent) in an Applied Biosystems

StepOne Plus real-time PCR machine. The expression levels of the following genes were detected using the following sets of primers: *Axin2* FW: 5'-AGCCTAAAGGTCTTATGTGG-3' and RV: 5'-ATGGAATCGTCGGTCAGT-3', *Osterix* (*Sp7*) FW: 5'-TCTGCTTGAGGAAGAAGCTC-3' and RV: 5'-TCCATTGGTGCTTGAGAAGG-3', *Gapdh* FW: 5'-CCAGTATGACTCCACTCACG-3' and RV: 5'-GACTCCACGACATACTCAGC-3'. The expression levels of the genes of interest were normalized to *Gapdh* expression levels for each particular sample.

#### *RNA sequencing*

Total RNA was isolated using Qiagen RNeasy Mini kit. Each biological replicate was created by pooling suture-derived cells of at least three mice. Three or four independent biological replicates were conducted for the conditions tested. NGS libraries were generated from 500 ng input total RNA with the Lexogen-QuantSeq 3' mRNA-Seq Library Prep Kit FWD for Illumina, and run on Illumina 500 on 1 x 150 Flowcells.

Fastq files from Illumina-BaseSpace were mapped to the mm10 genome (iGenomes UCSC/mm10) using hisat2 version 2.1.0 (--score-min L 0,-0.5) (84). Gene counts were computed with htseq-count (-s yes, version 0.11.2) (85). Differential analysis was performed with edgeR (3.24.3) (86, 87). Genes with cpm > 2 in at least 3 samples were included in the analysis. Samples were normalized by TMM. Sample grouping for the Design matrix was performed by one combined factor, which took into account ERF status, (plus =wt cells, minus=ERF KD cells) coupled to differentiation status (fresh=freshly harvested, LIF=long-term expanded or osteo=osteogenic induced), including also batch effect correction (model.matrix(~0+ERFstatus.DIFFstatus+batch)). Differential analyses were performed by likelihood ratio tests using the estimated negative binomial common dispersion. Sequencing data are deposited at <https://www.ncbi.nlm.nih.gov/sra?term=PRJNA664970>

#### *Single cell correlation analysis*

Count matrices of scRNA sequencing data were first analyzed filtered following the quality assessment suggested by Harvard Chan Bioinformatics Core ([https://hbctraining.github.io/scRNA-seq/lessons/04\\_SC\\_quality\\_control.html](https://hbctraining.github.io/scRNA-seq/lessons/04_SC_quality_control.html)) and normalized following Seurat's default method (88). Features that were not detected in at least 2% of the cells were also eliminated to improve reliability of a possible correlation. Gene correlation with the false discovery rate at 0.05 significance, were calculated using the corr.test function (89) in the R statistical environment (90). The a Wilcoxon rank sum test, as implemented in the wilcox.test function from the stats package (90), was used to further evaluate differences in the distribution of the correlated gene in cells expressing the target gene or not. Enrichment analysis sets for *Mus musculus* was performed with the gprofiler2 package (91), with a statistical domain size comprising of genes that have at least one annotation and with the g:SCS multiple testing correction method. The whole workflow was implemented in R version 3.6.1 (2019-07-05). Clustering of correlated gene sets across different scRNA data sets and target genes was visualized with metascape web tool (53) and ComplexHeatmap (92). The analysis software and genelist files are deposited at [https://github.com/mpaltsai/iRNA\\_project](https://github.com/mpaltsai/iRNA_project)

### *Statistical analysis*

All experiments had a minimum of two biological replicates and two experimental replicates for each. At least 3-4 sibling mice were used to derive each biological dsMSC sample. Variation among experimental replicates was minimal. Equal number for of experimental replicates was used for each biological replicate in each experiment. The data, unless otherwise stated, were analyzed using SPSS software. Unpaired (two-sided) t-test was conducted for comparisons between two groups and one-way Analysis of Variance (ANOVA) was performed for multiple comparisons, followed by post hoc Dunnett's two-sided test according to the experimental requirements. Levels of significance: \*  $p < 0.05$ , \*\*  $p < 0.01$ , \*\*\*  $p < 0.001$ .

### ***Acknowledgments***



We are grateful to the IMBB Animal House and Gene Targeting Facility personnel for mouse breeding and maintenance and the Genomics Facility personnel for high throughput RNA sequencing. This work was supported by an IKY-SIEMENS #AP2788 and a GSRT Bioimaging-GR grant #KA4937 to GM, an Onassis Foundation Fellowship #GZM 008-1 to AV. Work in Oxford was supported by Action Medical Research (GN2483; SRFT), the MRC through the WIMM Strategic Alliance (G0902418 and MC\_UU\_12025), National Institute for Health Research, and Wellcome (Investigator Award 102731 to Andrew OM Wilkie, and Project Grant 093329 to Andrew OM Wilkie and SRFT). For the purpose of open access, the author has applied a CC BY public copyright license to any Author Accepted Manuscript version arising from this submission.

### **Conflicts of Interest**

The authors declare no conflict of interest

### **References**

1. **Morriss-Kay GM, Wilkie AO.** 2005. Growth of the normal skull vault and its alteration in craniosynostosis: insights from human genetics and experimental studies. *J Anat* **207**:637-653.
2. **Opperman LA.** 2000. Cranial sutures as intramembranous bone growth sites. *Dev Dyn* **219**:472-485.
3. **Debnath S, Yallowitz AR, McCormick J, Lalani S, Zhang T, Xu R, Li N, Liu Y, Yang YS, Eiseman M, Shim JH, Hameed M, Healey JH, Bostrom MP, Landau DA, Greenblatt MB.** 2018. Discovery of a periosteal stem cell mediating intramembranous bone formation. *Nature* **562**:133-139.
4. **Zhao H, Feng J, Ho TV, Grimes W, Urata M, Chai Y.** 2015. The suture provides a niche for mesenchymal stem cells of craniofacial bones. *Nat Cell Biol* **17**:386-396.
5. **Lana-Elola E, Rice R, Grigoriadis AE, Rice DP.** 2007. Cell fate specification during calvarial bone and suture development. *Dev Biol* **311**:335-346.
6. **Fragale A, Tartaglia M, Bernardini S, Di Stasi AM, Di Rocco C, Velardi F, Teti A, Battaglia PA, Migliaccio S.** 1999. Decreased proliferation and altered differentiation in osteoblasts from genetically and clinically distinct craniosynostotic disorders. *Am J Pathol* **154**:1465-1477.
7. **Twigg SR, Wilkie AO.** 2015. A Genetic-Pathophysiological Framework for Craniosynostosis. *Am J Hum Genet* **97**:359-377.
8. **Johnson D, Wilkie AO.** 2011. Craniosynostosis. *Eur J Hum Genet* **19**:369-376.
9. **Yin L, Du X, Li C, Xu X, Chen Z, Su N, Zhao L, Qi H, Li F, Xue J, Yang J, Jin M, Deng C, Chen L.** 2008. A Pro253Arg mutation in fibroblast growth factor receptor 2 (Fgfr2) causes skeleton malformation mimicking human Apert syndrome by affecting both chondrogenesis and osteogenesis. *Bone* **42**:631-643.

10. **Shukla V, Coumoul X, Wang RH, Kim HS, Deng CX.** 2007. RNA interference and inhibition of MEK-ERK signaling prevent abnormal skeletal phenotypes in a mouse model of craniosynostosis. *Nat Genet* **39**:1145-1150.
11. **Pfaff MJ, Xue K, Li L, Horowitz MC, Steinbacher DM, Eswarakumar JVP.** 2016. FGFR2c-mediated ERK-MAPK activity regulates coronal suture development. *Dev Biol* **415**:242-250.
12. **Vogiatzi A, Mavrothalassitis G.** 2019. Craniofacial, orofacial and dental disorders: the role of the RAS/ERK pathway. *Expert Rev Mol Med* **21**:e2.
13. **Miraoui H, Marie PJ.** 2010. Fibroblast growth factor receptor signaling crosstalk in skeletogenesis. *Sci Signal* **3**:re9.
14. **Ornitz DM, Marie PJ.** 2015. Fibroblast growth factor signaling in skeletal development and disease. *Genes Dev* **29**:1463-1486.
15. **Le Gallic L, Sgouras D, Beal G, Jr., Mavrothalassitis G.** 1999. Transcriptional repressor ERF is a Ras/mitogen-activated protein kinase target that regulates cellular proliferation. *Mol Cell Biol* **19**:4121-4133.
16. **Le Gallic L, Virgilio L, Cohen P, Biteau B, Mavrothalassitis G.** 2004. ERF nuclear shuttling, a continuous monitor of Erk activity that links it to cell cycle progression. *Mol Cell Biol* **24**:1206-1218.
17. **Papadaki C, Alexiou M, Cecena G, Verykokakis M, Bilitou A, Cross JC, Oshima RG, Mavrothalassitis G.** 2007. Transcriptional repressor erf determines extraembryonic ectoderm differentiation. *Mol Cell Biol* **27**:5201-5213.
18. **Peraki I, Palis J, Mavrothalassitis G.** 2017. The Ets2 Repressor Factor (Erf) Is Required for Effective Primitive and Definitive Hematopoiesis. *Mol Cell Biol* **37**.
19. **Glass GE, O'Hara J, Canham N, Cilliers D, Dunaway D, Fenwick AL, Jeelani NO, Johnson D, Lester T, Lord H, Morton JEV, Nishikawa H, Noons P, Schwiebert K, Shipster C, Taylor-Beadling A, Twigg SRF, Vasudevan P, Wall SA, Wilkie AOM, Wilson LC.** 2019. ERF-related craniosynostosis: The phenotypic and developmental profile of a new craniosynostosis syndrome. *Am J Med Genet A* **179**:615-627.
20. **Twigg SR, Vorgia E, McGowan SJ, Peraki I, Fenwick AL, Sharma VP, Allegra M, Zaragkoulias A, Sadighi Akha E, Knight SJ, Lord H, Lester T, Izatt L, Lampe AK, Mohammed SN, Stewart FJ, Verloes A, Wilson LC, Healy C, Sharpe PT, Hammond P, Hughes J, Taylor S, Johnson D, Wall SA, Mavrothalassitis G, Wilkie AO.** 2013. Reduced dosage of ERF causes complex craniosynostosis in humans and mice and links ERK1/2 signaling to regulation of osteogenesis. *Nat Genet* **45**:308-313.
21. **Clagett-Dame M, DeLuca HF.** 2002. The role of vitamin A in mammalian reproduction and embryonic development. *Annu Rev Nutr* **22**:347-381.
22. **Duester G.** 2008. Retinoic acid synthesis and signaling during early organogenesis. *Cell* **134**:921-931.
23. **Dersch H, Zile MH.** 1993. Induction of normal cardiovascular development in the vitamin A-deprived quail embryo by natural retinoids. *Dev Biol* **160**:424-433.
24. **Dickman ED, Thaller C, Smith SM.** 1997. Temporally-regulated retinoic acid depletion produces specific neural crest, ocular and nervous system defects. *Development* **124**:3111-3121.
25. **Lohnes D, Mark M, Mendelsohn C, Dolle P, Dierich A, Gorry P, Gansmuller A, Chambon P.** 1994. Function of the retinoic acid receptors (RARs) during development (I). Craniofacial and skeletal abnormalities in RAR double mutants. *Development* **120**:2723-2748.
26. **Mendelsohn C, Lohnes D, Decimo D, Lufkin T, LeMeur M, Chambon P, Mark M.** 1994. Function of the retinoic acid receptors (RARs) during development (II). Multiple abnormalities at various stages of organogenesis in RAR double mutants. *Development* **120**:2749-2771.

27. **Martinez-Morales PL, Diez del Corral R, Olivera-Martinez I, Quiroga AC, Das RM, Barbas JA, Storey KG, Morales AV.** 2011. FGF and retinoic acid activity gradients control the timing of neural crest cell emigration in the trunk. *J Cell Biol* **194**:489-503.
28. **Sirbu IO, Zhao X, Duester G.** 2008. Retinoic acid controls heart anteroposterior patterning by down-regulating *Isl1* through the *Fgf8* pathway. *Dev Dyn* **237**:1627-1635.
29. **Geelen JA.** 1979. Hypervitaminosis A induced teratogenesis. *CRC Crit Rev Toxicol* **6**:351-375.
30. **Gardner JS, Guyard-Boileau B, Alderman BW, Fernbach SK, Greene C, Mangione EJ.** 1998. Maternal exposure to prescription and non-prescription pharmaceuticals or drugs of abuse and risk of craniosynostosis. *Int J Epidemiol* **27**:64-67.
31. **Yip JE, Kokich VG, Shepard TH.** 1980. The effect of high doses of retinoic acid on prenatal craniofacial development in *Macaca nemestrina*. *Teratology* **21**:29-38.
32. **Laue K, Pogoda HM, Daniel PB, van Haeringen A, Alanay Y, von Ameln S, Rachwalski M, Morgan T, Gray MJ, Breuning MH, Sawyer GM, Sutherland-Smith AJ, Nikkels PG, Kubisch C, Bloch W, Wollnik B, Hammerschmidt M, Robertson SP.** 2011. Craniosynostosis and multiple skeletal anomalies in humans and zebrafish result from a defect in the localized degradation of retinoic acid. *Am J Hum Genet* **89**:595-606.
33. **Leitch VD, Dwivedi PP, Anderson PJ, Powell BC.** 2013. Retinol-binding protein 4 downregulation during osteogenesis and its localization to non-endocytic vesicles in human cranial suture mesenchymal cells suggest a novel tissue function. *Histochem Cell Biol* **139**:75-87.
34. **Maclean G, Dolle P, Petkovich M.** 2009. Genetic disruption of *CYP26B1* severely affects development of neural crest derived head structures, but does not compromise hindbrain patterning. *Dev Dyn* **238**:732-745.
35. **Ferguson JW, Devarajan M, Atit RP.** 2018. Stage-specific roles of *Ezh2* and Retinoic acid signaling ensure calvarial bone lineage commitment. *Dev Biol* **443**:173-187.
36. **Draut H, Liebenstein T, Begemann G.** 2019. New Insights into the Control of Cell Fate Choices and Differentiation by Retinoic Acid in Cranial, Axial and Caudal Structures. *Biomolecules* **9**.
37. **Xu Y, Malladi P, Chiou M, Longaker MT.** 2007. Isolation and characterization of posterofrontal/sagittal suture mesenchymal cells in vitro. *Plast Reconstr Surg* **119**:819-829.
38. **Aubin JE, Liu F, Malaval L, Gupta AK.** 1995. Osteoblast and chondroblast differentiation. *Bone* **17**:77S-83S.
39. **Mercader N, Leonardo E, Piedra ME, Martinez AC, Ros MA, Torres M.** 2000. Opposing RA and FGF signals control proximodistal vertebrate limb development through regulation of *Meis* genes. *Development* **127**:3961-3970.
40. **Probst S, Kraemer C, Demougin P, Sheth R, Martin GR, Shiratori H, Hamada H, Iber D, Zeller R, Zuniga A.** 2011. *SHH* propagates distal limb bud development by enhancing *CYP26B1*-mediated retinoic acid clearance via AER-FGF signalling. *Development* **138**:1913-1923.
41. **Deng MJ, Jin Y, Shi JN, Lu HB, Liu Y, He DW, Nie X, Smith AJ.** 2004. Multilineage differentiation of ectomesenchymal cells isolated from the first branchial arch. *Tissue Eng* **10**:1597-1606.
42. **Malaval L, Gupta AK, Aubin JE.** 1995. Leukemia inhibitory factor inhibits osteogenic differentiation in rat calvaria cell cultures. *Endocrinology* **136**:1411-1418.
43. **Maruyama T, Jeong J, Sheu TJ, Hsu W.** 2016. Stem cells of the suture mesenchyme in craniofacial bone development, repair and regeneration. *Nat Commun* **7**:10526.
44. **Dominici M, Le Blanc K, Mueller I, Slaper-Cortenbach I, Marini F, Krause D, Deans R, Keating A, Prockop D, Horwitz E.** 2006. Minimal criteria for defining multipotent

- mesenchymal stromal cells. The International Society for Cellular Therapy position statement. *Cytotherapy* **8**:315-317.
45. **Meirelles Lda S, Nardi NB.** 2003. Murine marrow-derived mesenchymal stem cell: isolation, in vitro expansion, and characterization. *Br J Haematol* **123**:702-711.
  46. **Zhu H, Guo ZK, Jiang XX, Li H, Wang XY, Yao HY, Zhang Y, Mao N.** 2010. A protocol for isolation and culture of mesenchymal stem cells from mouse compact bone. *Nat Protoc* **5**:550-560.
  47. **Verykokakis M, Papadaki C, Vorgia E, Le Gallic L, Mavrothalassitis G.** 2007. The RAS-dependent ERF control of cell proliferation and differentiation is mediated by c-Myc repression. *J Biol Chem* **282**:30285-30294.
  48. **Subramanian A, Tamayo P, Mootha VK, Mukherjee S, Ebert BL, Gillette MA, Paulovich A, Pomeroy SL, Golub TR, Lander ES, Mesirov JP.** 2005. Gene set enrichment analysis: a knowledge-based approach for interpreting genome-wide expression profiles. *Proc Natl Acad Sci U S A* **102**:15545-15550.
  49. **Brinkley JF, Fisher S, Harris MP, Holmes G, Hooper JE, Jabs EW, Jones KL, Kesselman C, Klein OD, Maas RL, Marazita ML, Selleri L, Spritz RA, van Bakel H, Visel A, Williams TJ, Wysocka J, FaceBase C, Chai Y.** 2016. The FaceBase Consortium: a comprehensive resource for craniofacial researchers. *Development* **143**:2677-2688.
  50. **Holmes G, Gonzalez-Reiche AS, Lu N, Zhou X, Rivera J, Kriti D, Sebra R, Williams AA, Donovan MJ, Potter SS, Pinto D, Zhang B, van Bakel H, Jabs EW.** 2020. Integrated Transcriptome and Network Analysis Reveals Spatiotemporal Dynamics of Calvarial Suturogenesis. *Cell Rep* **32**:107871.
  51. **Falker-Gieske C, Mott A, Franzenburg S, Tetens J.** 2021. Multi-species transcriptome meta-analysis of the response to retinoic acid in vertebrates and comparative analysis of the effects of retinol and retinoic acid on gene expression in LMH cells. *BMC Genomics* **22**:146.
  52. **Terranova C, Narla ST, Lee YW, Bard J, Parikh A, Stachowiak EK, Tzanakakis ES, Buck MJ, Birkaya B, Stachowiak MK.** 2015. Global Developmental Gene Programing Involves a Nuclear Form of Fibroblast Growth Factor Receptor-1 (FGFR1). *PLoS One* **10**:e0123380.
  53. **Zhou Y, Zhou B, Pache L, Chang M, Khodabakhshi AH, Tanaseichuk O, Benner C, Chanda SK.** 2019. Metascape provides a biologist-oriented resource for the analysis of systems-level datasets. *Nat Commun* **10**:1523.
  54. **Spoorendonk KM, Peterson-Maduro J, Renn J, Trowe T, Kranenbarg S, Winkler C, Schulte-Merker S.** 2008. Retinoic acid and Cyp26b1 are critical regulators of osteogenesis in the axial skeleton. *Development* **135**:3765-3774.
  55. **Roberts C.** 2020. Regulating Retinoic Acid Availability during Development and Regeneration: The Role of the CYP26 Enzymes. *J Dev Biol* **8**.
  56. **Pricola KL, Kuhn NZ, Haleem-Smith H, Song Y, Tuan RS.** 2009. Interleukin-6 maintains bone marrow-derived mesenchymal stem cell stemness by an ERK1/2-dependent mechanism. *J Cell Biochem* **108**:577-588.
  57. **Song HM, Nacamuli RP, Xia W, Bari AS, Shi YY, Fang TD, Longaker MT.** 2005. High-dose retinoic acid modulates rat calvarial osteoblast biology. *J Cell Physiol* **202**:255-262.
  58. **James AW, Levi B, Xu Y, Carre AL, Longaker MT.** 2010. Retinoic acid enhances osteogenesis in cranial suture-derived mesenchymal cells: potential mechanisms of retinoid-induced craniosynostosis. *Plast Reconstr Surg* **125**:1352-1361.
  59. **Gonzalez-Quevedo R, Lee Y, Poss KD, Wilkinson DG.** 2010. Neuronal regulation of the spatial patterning of neurogenesis. *Dev Cell* **18**:136-147.
  60. **Bao X, Zhang X, Wang L, Wang Z, Huang J, Zhang Q, Ye Y, Liu Y, Chen D, Zuo Y, Liu Q, Xu P, Huang B, Fang J, Lao J, Feng X, Li Y, Kurita R, Nakamura Y, Yu W, Ju**

- C, Huang C, Mohandas N, Li D, Zhao C, Xu X. 2021. Epigenetic inactivation of ERF reactivates gamma-globin expression in beta-thalassemia. *Am J Hum Genet* doi:10.1016/j.ajhg.2021.03.005.
61. Bose R, Karthaus WR, Armenia J, Abida W, Iaquinta PJ, Zhang Z, Wongvipat J, Wasmuth EV, Shah N, Sullivan PS, Doran MG, Wang P, Patruno A, Zhao Y, Zheng D, Schultz N, Sawyers CL. 2017. ERF mutations reveal a balance of ETS factors controlling prostate oncogenesis. *Nature* **546**:671-675.
  62. Mayor-Ruiz C, Olbrich T, Drosten M, Lecona E, Vega-Sendino M, Ortega S, Dominguez O, Barbacid M, Ruiz S, Fernandez-Capetillo O. 2018. ERF deletion rescues RAS deficiency in mouse embryonic stem cells. *Genes Dev* **32**:568-576.
  63. Sumarsono SH, Wilson TJ, Tymms MJ, Venter DJ, Corrick CM, Kola R, Lahoud MH, Papas TS, Seth A, Kola I. 1996. Down's syndrome-like skeletal abnormalities in Ets2 transgenic mice. *Nature* **379**:534-537.
  64. Vary CP, Li V, Raouf A, Kitching R, Kola I, Franceschi C, Venanzoni M, Seth A. 2000. Involvement of Ets transcription factors and targets in osteoblast differentiation and matrix mineralization. *Exp Cell Res* **257**:213-222.
  65. Lomri A, Lemonnier J, Hott M, de Parseval N, Lajeunie E, Munnich A, Renier D, Marie PJ. 1998. Increased calvaria cell differentiation and bone matrix formation induced by fibroblast growth factor receptor 2 mutations in Apert syndrome. *J Clin Invest* **101**:1310-1317.
  66. Holmes G, Rothschild G, Roy UB, Deng CX, Mansukhani A, Basilico C. 2009. Early onset of craniosynostosis in an Apert mouse model reveals critical features of this pathology. *Dev Biol* **328**:273-284.
  67. Teng CS, Ting MC, Farmer DT, Brockop M, Maxson RE, Crump JG. 2018. Altered bone growth dynamics prefigure craniosynostosis in a zebrafish model of Saethre-Chotzen syndrome. *Elife* **7**.
  68. Matsushita T, Chan YY, Kawanami A, Balmes G, Landreth GE, Murakami S. 2009. Extracellular signal-regulated kinase 1 (ERK1) and ERK2 play essential roles in osteoblast differentiation and in supporting osteoclastogenesis. *Mol Cell Biol* **29**:5843-5857.
  69. Kyono A, Avishai N, Ouyang Z, Landreth GE, Murakami S. 2012. FGF and ERK signaling coordinately regulate mineralization-related genes and play essential roles in osteocyte differentiation. *J Bone Miner Metab* **30**:19-30.
  70. Tsang EJ, Wu B, Zuk P. 2018. MAPK signaling has stage-dependent osteogenic effects on human adipose-derived stem cells in vitro. *Connect Tissue Res* **59**:129-146.
  71. Weng Z, Wang C, Zhang C, Xu J, Chai Y, Jia Y, Han P, Wen G. 2019. All-Trans Retinoic Acid Promotes Osteogenic Differentiation and Bone Consolidation in a Rat Distraction Osteogenesis Model. *Calcif Tissue Int* **104**:320-330.
  72. Cruz ACC, Cardozo F, Magini RS, Simoes CMO. 2019. Retinoic acid increases the effect of bone morphogenetic protein type 2 on osteogenic differentiation of human adipose-derived stem cells. *J Appl Oral Sci* **27**:e20180317.
  73. Roa LA, Bloemen M, Carels CEL, Wagener F, Von den Hoff JW. 2019. Retinoic acid disrupts osteogenesis in pre-osteoblasts by down-regulating WNT signaling. *Int J Biochem Cell Biol* **116**:105597.
  74. Bi W, Gu Z, Zheng Y, Zhang X, Guo J, Wu G. 2013. Heterodimeric BMP-2/7 antagonizes the inhibition of all-trans retinoic acid and promotes the osteoblastogenesis. *PLoS One* **8**:e78198.
  75. Lind T, Sundqvist A, Hu L, Pejler G, Andersson G, Jacobson A, Melhus H. 2013. Vitamin a is a negative regulator of osteoblast mineralization. *PLoS One* **8**:e82388.
  76. Cristofalo VJ, Allen RG, Pignolo RJ, Martin BG, Beck JC. 1998. Relationship between donor age and the replicative lifespan of human cells in culture: a reevaluation. *Proc Natl Acad Sci U S A* **95**:10614-10619.

77. **Sasaki M, Abe R, Fujita Y, Ando S, Inokuma D, Shimizu H.** 2008. Mesenchymal stem cells are recruited into wounded skin and contribute to wound repair by transdifferentiation into multiple skin cell type. *J Immunol* **180**:2581-2587.
78. **Kastrinaki MC, Andreakou I, Charbord P, Papadaki HA.** 2008. Isolation of human bone marrow mesenchymal stem cells using different membrane markers: comparison of colony/cloning efficiency, differentiation potential, and molecular profile. *Tissue Eng Part C Methods* **14**:333-339.
79. **Russell KC, Phinney DG, Lacey MR, Barrilleaux BL, Meyertholen KE, O'Connor KC.** 2010. In vitro high-capacity assay to quantify the clonal heterogeneity in trilineage potential of mesenchymal stem cells reveals a complex hierarchy of lineage commitment. *Stem Cells* **28**:788-798.
80. **Gregory CA, Gunn WG, Peister A, Prockop DJ.** 2004. An Alizarin red-based assay of mineralization by adherent cells in culture: comparison with cetylpyridinium chloride extraction. *Anal Biochem* **329**:77-84.
81. **Gruber HE, Somayaji S, Riley F, Hoelscher GL, Norton HJ, Ingram J, Hanley EN, Jr.** 2012. Human adipose-derived mesenchymal stem cells: serial passaging, doubling time and cell senescence. *Biotech Histochem* **87**:303-311.
82. **Nicoletti I, Migliorati G, Pagliacci MC, Grignani F, Riccardi C.** 1991. A rapid and simple method for measuring thymocyte apoptosis by propidium iodide staining and flow cytometry. *J Immunol Methods* **139**:271-279.
83. **Morgan DM.** 1998. Tetrazolium (MTT) assay for cellular viability and activity. *Methods Mol Biol* **79**:179-183.
84. **Kim D, Langmead B, Salzberg SL.** 2015. HISAT: a fast spliced aligner with low memory requirements. *Nat Methods* **12**:357-360.
85. **Anders S, Pyl PT, Huber W.** 2015. HTSeq--a Python framework to work with high-throughput sequencing data. *Bioinformatics* **31**:166-169.
86. **Robinson MD, McCarthy DJ, Smyth GK.** 2010. edgeR: a Bioconductor package for differential expression analysis of digital gene expression data. *Bioinformatics* **26**:139-140.
87. **McCarthy DJ, Chen Y, Smyth GK.** 2012. Differential expression analysis of multifactor RNA-Seq experiments with respect to biological variation. *Nucleic Acids Res* **40**:4288-4297.
88. **Stuart T, Butler A, Hoffman P, Hafemeister C, Papalexi E, Mauck WM, 3rd, Hao Y, Stoeckius M, Smibert P, Satija R.** 2019. Comprehensive Integration of Single-Cell Data. *Cell* **177**:1888-1902 e1821.
89. **Revelle W.** 2019. psych: Procedures for Psychological, Psychometric, and Personality Research. Northwestern University, Evanston, Illinois.
90. **Team RC.** 2019. R: A Language and Environment for Statistical Computing. R Foundation for Statistical Computing, Vienna, Austria.
91. **Raudvere U, Kolberg L, Kuzmin I, Arak T, Adler P, Peterson H, Vilo J.** 2019. g:Profiler: a web server for functional enrichment analysis and conversions of gene lists (2019 update). *Nucleic Acids Res* **47**:W191-W198.
92. **Gu Z, Eils R, Schlesner M.** 2016. Complex heatmaps reveal patterns and correlations in multidimensional genomic data. *Bioinformatics* **32**:2847-2849.

## Figure legends

**Figure 1: Characterization of LIF-selected suture-derived mesenchymal cells expanded in culture for 8 population doublings (PDs).** A) A schematic representation and timeline of the cell isolation, culture and characterization process. B) Phase-contrast image of suture-derived wild-type cells displaying a fibroblastoid morphology. C) *Axin2* and *Osterix* mRNA levels normalized to *Gapdh* as determined by qPCR in suture cells of the indicated population doubling level (PD). Data were analyzed with one-way ANOVA followed by Dunnett's (two-sided) test to compare all groups against control group (PD 0). \*  $p < 0.05$ , \*\*  $p < 0.01$ , \*\*\*  $p < 0.001$ . D) Flow-cytometric analysis of cells for mesenchymal stem cell (MSC) markers (CD44, CD90, CD29, Sca1, CD105) and hematopoietic/ endothelial markers (CD45, CD34, CD31). Filled histograms indicate the unlabelled cells used as negative controls. E) Cells were induced to differentiate towards osteocytes, adipocytes and chondrocytes, and stained respectively with Alizarin Red S, Oil Red O and Alcian blue/ Hematoxylin. Scale bars represent 100  $\mu\text{m}$ , 50  $\mu\text{m}$  and 20  $\mu\text{m}$  respectively. F) Graph showing the population doublings over time in culture for LIF-expanded suture mesenchymal cells. Each measurement (point in graph) has been performed at the end of each passage.

**Figure 2: *Erf* insufficiency compromises the ability of sdMSCs to mineralize.** A) Frequency in each of the cell cycle phases of cells growing in maintenance conditions as determined by propidium iodide staining and flow cytometry. B) Doubling time in hours of *Erf*<sup>loxP/+</sup> and *Erf*<sup>loxP/-</sup> sdMSCs at the indicated population doubling levels (PDs). C-E) sdMSCs were induced to differentiate along the chondrogenic lineage for 21 days (C), the adipogenic lineage for 21 days (D) and the osteogenic lineage for 28 days (E) and stained respectively with Alcian blue & Hematoxylin, Oil Red O and Alizarin Red S. Scale bars represent 10  $\mu\text{m}$ , 50  $\mu\text{m}$  and 100  $\mu\text{m}$ , respectively. F) Measurements of the Alizarin Red S dye extracted from the cells after 28 days of osteogenic differentiation. Three independent biological experiments were conducted and the statistical analysis was performed using an unpaired t-test with two-tailed distribution. \*  $p < 0.05$

**Figure 3: Freshly isolated suture-derived Erf-insufficient cells display altered differentiation potential.** A) The initial heterogeneous population of cells was induced to differentiate along the osteogenic lineage for 28 days and stained with Alizarin Red S for calcium deposits. B) Quantification of Alizarin Red S levels after extraction from culture wells at the indicated time-points of differentiation. C) Cells differentiating towards chondrocytes for 21 days stained with Alcian blue and Hematoxylin. D) Cells differentiating towards adipocytes for 7 days stained with Oil Red O. E) The total number of cells in adipocyte differentiation was determined by Hoechst-33342 staining of the nuclei. Statistical analysis was performed using a t-test with two-tailed distribution. \*  $p < 0.05$ , \*\*  $p < 0.01$

**Figure 4: Extensive transcriptional differences between growth conditions but not genotypes.** A) RNA was collected from suture derived (picture on top) freshly isolated suture cells cultured for 7 days ("fresh [F]" - right), sdMSCs cultured for 8 PDs in maintenance medium ("self-renewal [L]" - left) and sdMSCs of 8 PDs induced with osteogenic differentiation medium for 24h ("osteo-diff [O]" - middle). At least 3-4 mice were used per genotype for each of the above conditions tested per experiment and at least 4 independent experiments were conducted. B) Unsupervised clustering of gene expression experiment from Erf-competent  $Erf^{loxP/+}$  (P/+) and Erf-insufficient  $Erf^{loxP/-}$  (P/-) cells, indicating no genotype-specific associations. Self renewal: sdMSCs in self renewal media, Osteo differentiation: sdMSCs 24 h in osteogenic differentiation medium, Fresh cells: freshly isolated suture-derived cells. C) Heatmaps based on the 60 most differentially expressed genes of the indicated comparison, showing a clear clustering between conditions but not genotypes. Self renewal: sdMSCs in self renewal media, Osteo Diff: sdMSCs 24 h in osteogenic differentiation medium, Fresh: freshly isolated suture-derived cells, P/+: Erf-competent ( $Erf^{loxP/+}$ ) cells, P/-: Erf-insufficient ( $Erf^{loxP/-}$ ) cells.

**Figure 5: Transcriptome analysis indicates a deficit of extracellular matrix- and ossification- related genes in Erf-insufficient cells.** A, B) The limited number of genes found significantly decreased in Erf-insufficient cells compared to Erf-



competent (Table 1), were analyzed with the GSEA program and visualized with ComplexHeatmap in the R environment. The significance of top 10 categories enriched in the query genes for the sdMSCs in osteogenic differentiation (A) and for the initial heterogeneous suture cell population (freshly isolated cells) (B) is shown. C) Differentially expressed genes identified by transcriptome analysis (Supplementary Table 1) of sdMSCs (L), sdMSCs growing in osteogenic differentiation media for 24 h (O) and freshly isolated suture cells (F), from Erf-competent (*Erf*<sup>loxP/+</sup>; “plus”) and Erf-insufficient (*Erf*<sup>loxP/-</sup>; “minus”) animals, were clustered based on their ontology with the Metascape program. L-O comm.: genes found differentially expressed during the 24h induction of sdMSCs of both Erf-competent and Erf-insufficient cells. L-O plus: genes found differentially expressed during the 24h induction only in the Erf-competent sdMSCs. L-O minus: genes found differentially expressed during the 24h induction only in the Erf-insufficient sdMSCs. Respectively “L-F” indicates genes found differentially expressed between sdMSCs and freshly isolated cells and “O-F” between sdMSCs differentiating for 24h and freshly isolated cells. Red lettering indicates ossification related- and orange lettering differentiation- related ontologies. Only the top 20 categories are shown.

**Figure 6: *Erf* expression correlates with ossification- and extracellular matrix organization- related genes.** A) Genes found in mouse suture single cell RNA sequencing experiments (Supplementary Table 2) to correlate with *Erf* expression were clustered based on their ontology with the Metascape programme. P10: scRNA-seq data from P10 animals. E16.5: scRNA-seq data from E16.5 embryos. E18.5: scRNA-seq data from E18.5 embryos. B) as in A but with the addition of data from genes correlated with *Alpl*, *Fgfr2*, *Runx2*, *Sp7* and *Twist1* as markers for osteogenic differentiation stages. Red lettering indicates ossification related and orange differentiation related ontologies. Only the top 20 categories are shown.

**Figure 7: Retinoic acid reverts the osteogenic deficiency of *Erf*<sup>loxP/-</sup> sdMSCs.** A) Fold change in the expression level of *Erf* and *Cyp26b1* between Erf-competent and Erf-deficient cells in self-renewing sdMSCs (LIF), differentiating sdMSCs (Osteo) and

freshly derived suture cells (Fresh). B) Relative expression level of *Cyp26b1* compared to Erf-competent (*Erf<sup>loxP/+</sup>*) sdMSCs in proliferation media (LIF). C) Venn diagram showing genes differentially expressed during MSC differentiation for each genotype and genes found regulated in mESCs after retinoic acid treatment. The table above indicates the significance of the enrichment in RA-related genes. The number of common genes in each comparison is underlined. D) Analysis of genes associated with RA (underlined in C) via metascape, in relation to other transcription factors. Relative percentage of proliferating cells as estimated by BrdU incorporation during osteogenic differentiation of Erf-insufficient (*Erf<sup>loxP/-</sup>*) and Erf-competent (*Erf<sup>loxP/+</sup>*) sdMSCs. Data are derived from four independent biological experiments, each including two experimental replicates. F) Relative cell number during the same experiment as in (E). G) Cell numbers, as evaluated by formazan absorbance after 28 days in osteogenic differentiation medium in the presence or absence (C) of 0.5  $\mu$ M all-*trans* retinoic acid (RA). H) Calcification potential per cell as evaluated by the alizarin red s to formazan absorbance after 28 days of osteogenic differentiation in the presence or absence (C) of 0.5  $\mu$ M all-*trans* retinoic acid (RA). Data for A and B are derived from the RNA sequencing dataset and analyzed as described in the Materials and Methods section. The shown values have an FDR lower than 0.05. Data for G and H are from four experiments and the statistical analysis was performed in all cases using an unpaired t-test with two-tailed distribution. \*  $p < 0.05$ , \*\*  $p < 0.01$ , \*\*\*  $p < 0.001$ .

**Figure 8: Mechanism of Erf effect in the osteogenic differentiation of cranial suture mesenchymal stem/progenitor cells.** Erf, an FGF effector, affects the level of retinoic acid possibly through the RA catabolizing enzyme *Cyp26b1*. Decreased levels of Erf leads to increased levels of *Cyp26b1* which inturn decreases retinoic acid levels leading to reduced osteogenic differentiation and/or increased mesenchymal progenitor proliferation.

Table 1

Differentially expressed genes between the two genotypes in each culture condition. Genes different at least 1.5 fold with an FDR < 0.05 are shown.

Genes associated with Matrisome are shown in *italics* and the RA-related in **bold**.

sdMSC growing in				freshly isolated	
Self renewal (w/LIF)		Osteogenic differentiation		suture-derived cells	
Up in <i>Erf</i> <sup>P/+</sup>	Up in <i>Erf</i> <sup>P/-</sup>	Up in <i>Erf</i> <sup>P/+</sup>	Up in <i>Erf</i> <sup>P/-</sup>	Up in <i>Erf</i> <sup>P/+</sup>	Up in <i>Erf</i> <sup>P/-</sup>
Add3	4930511M06Rik	<i>Epb4.1l4a</i>	Acta1	Arf1	Ackr3
Amph	<b>Cyp26b1</b>	<i>Btbd2</i>	Actg2	<b>AW551984</b>	Ccl2
Epb4,1l4a	<b>Fst</b>	Cd34	Asb2	<i>Clec11a</i>	Ccl7
Erf	Styk1	<b>Col14a1</b>	Atp2b4	Dkk2	<b>Cyp26b1</b>
<b>Nell1</b>		<i>Cthrc1</i>	Cnn1	<i>Edil3</i>	Dynap
Nts		Cygb	<b>Cyp26b1</b>	Erf	F3
Ostn		Cyp2c29	Dmpk	<i>Gpc1</i>	Fbxl19
Slitrk6		Cyp2c54	Eng	<i>Igfbp5</i>	Gsto1
<b>Tmod2</b>		Cyp2d26	F2r	<i>Lum</i>	Id4
Zfp729a		<b>Emilin2</b>	<b>Fst</b>	Lyz1	<b>lrx1</b>
		Erf	Ldb3	Med12l	Lrrc32
		<i>Esm1</i>	<b>Lmod1</b>	Myof	Lrrk2
		F5	Lrrc58	<i>Ptn</i>	Ltbp2
		<b>Gfra1</b>	Mbp	<i>Sema3a</i>	<b>Lurap1l</b>
		<b>Gpx3</b>	Myh11	<i>Sema3e</i>	Mfap5
		H2afv	Pip4k2a	<b>Serpinb1a</b>	Ppap2b
		<i>Lrg1</i>	Plac8	Slc1a7	Rgs16
		Mgst1	Pnck	<i>Tgfb1</i>	Saal1
		Nav1	<b>Sh3bgr</b>	Zcchc5	Serpinb2
		<b>Rnpepl1</b>	Tagln		Sfrp1
		Saa2	Tbx18		Siglecg
		<b>Slc25a47</b>	Tnfaip2		Stc1
		Tmod2	Vwce		Tm4sf1
		Ttpa			<b>Twist2</b>
		Zfp738			

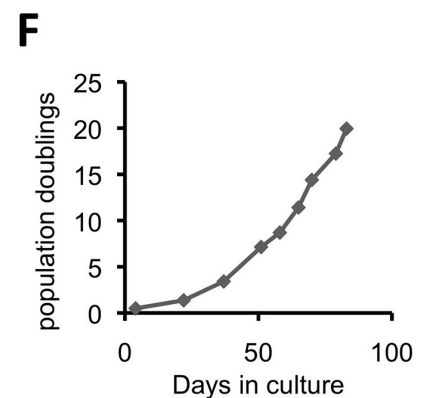
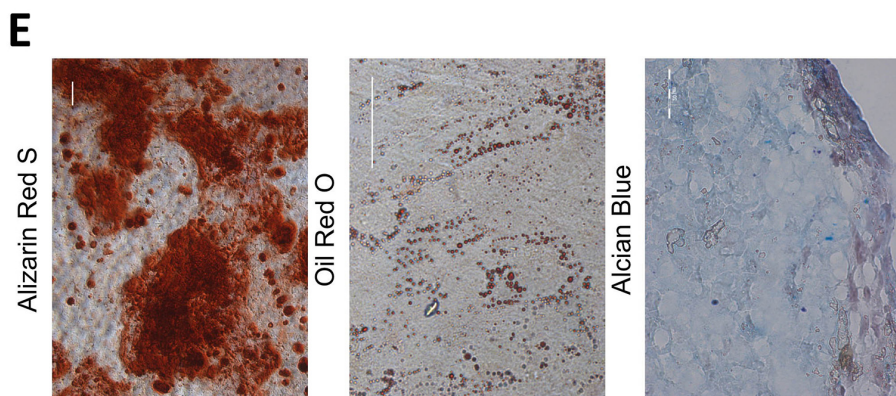
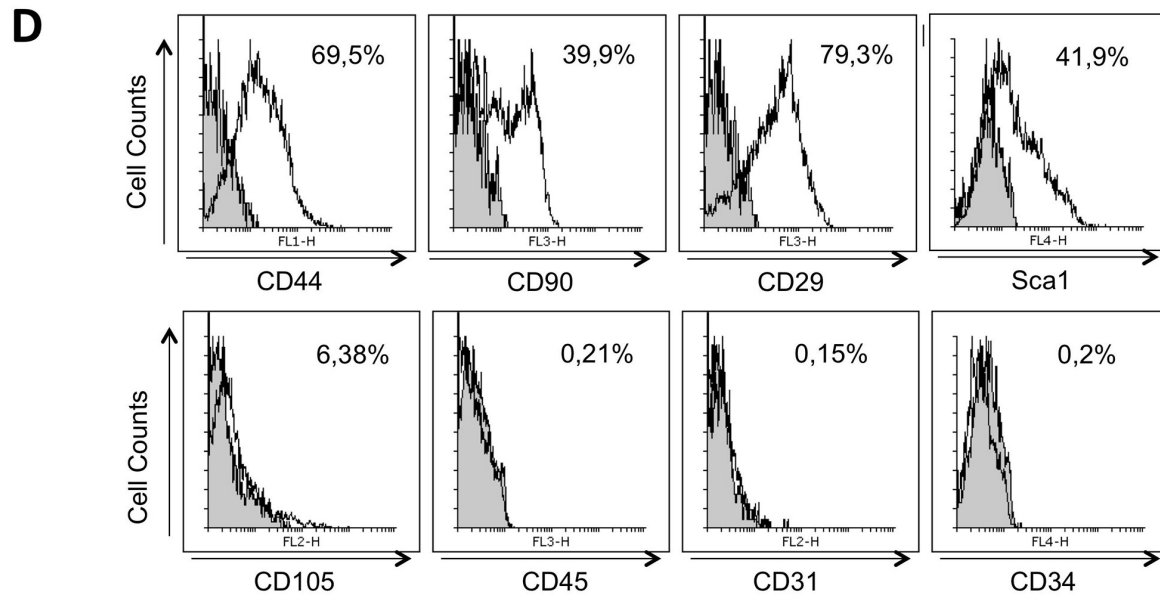
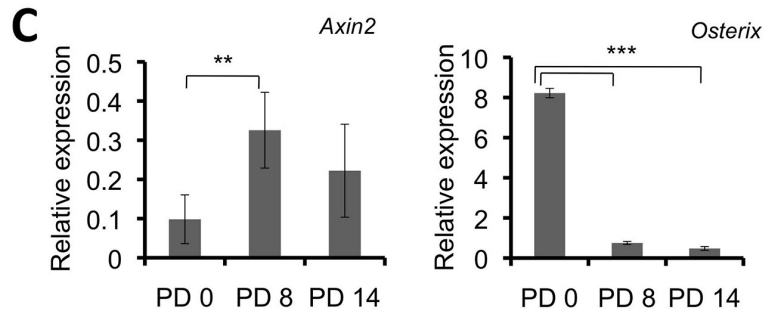
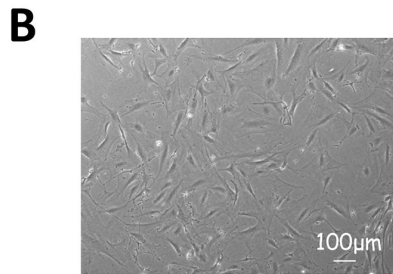
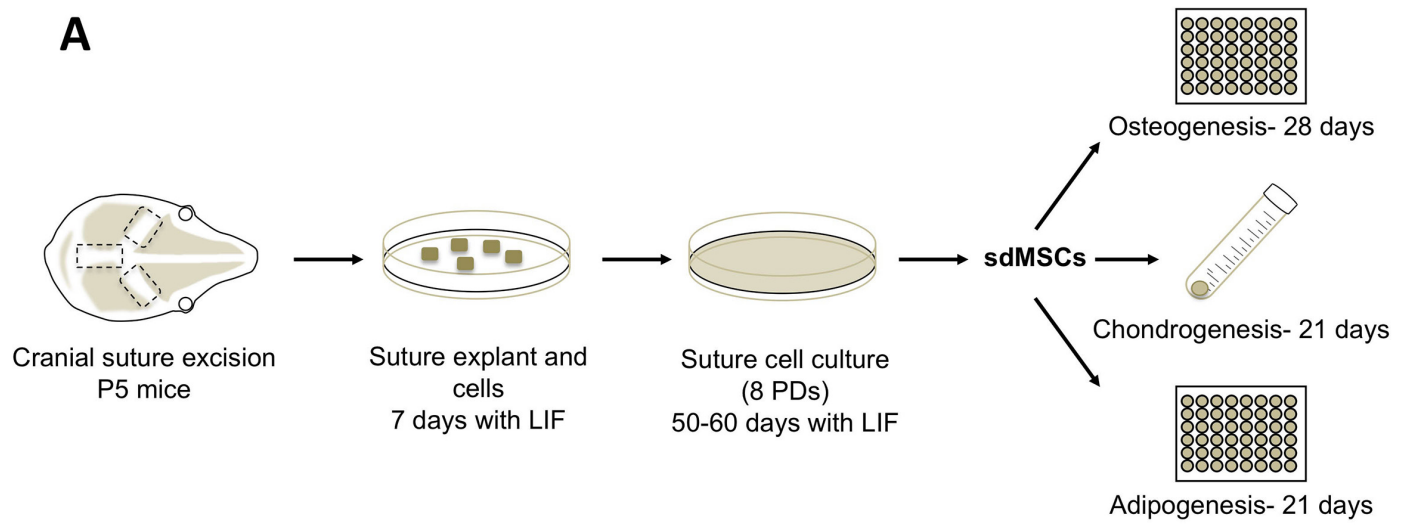
901

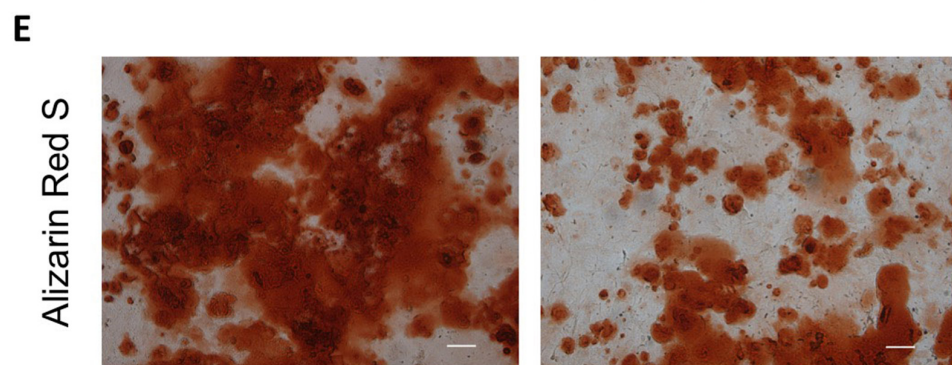
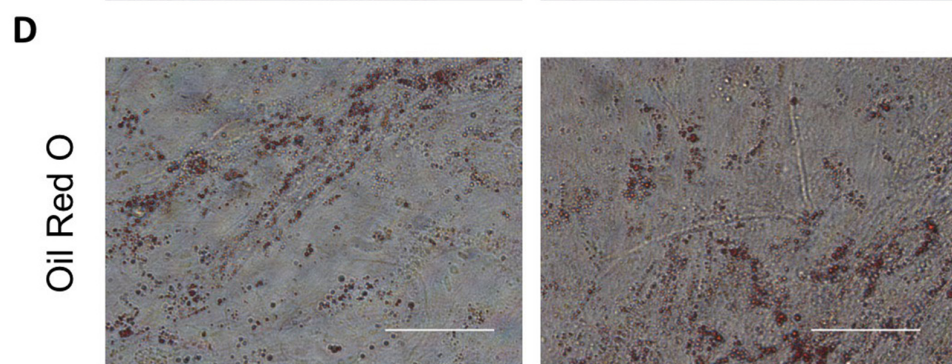
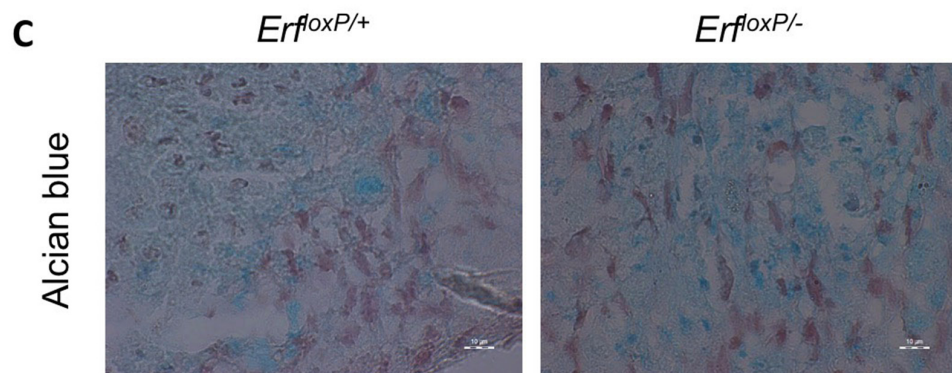
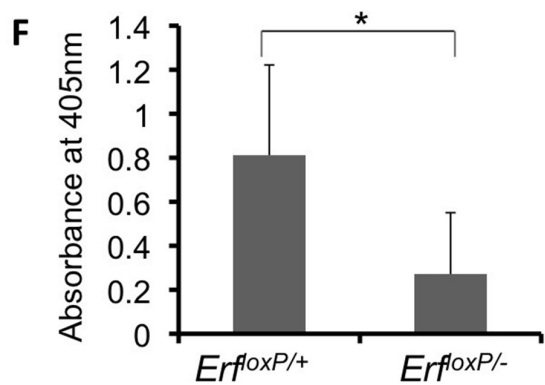
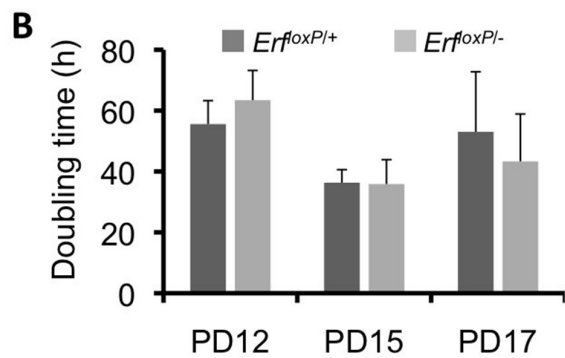
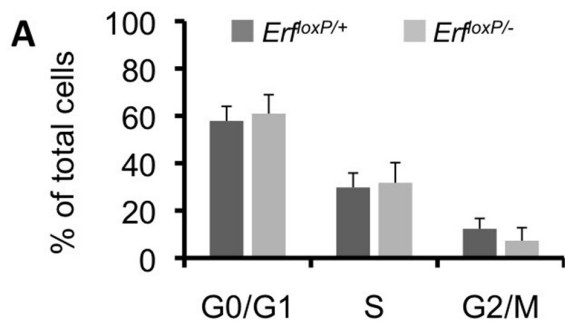
902

903

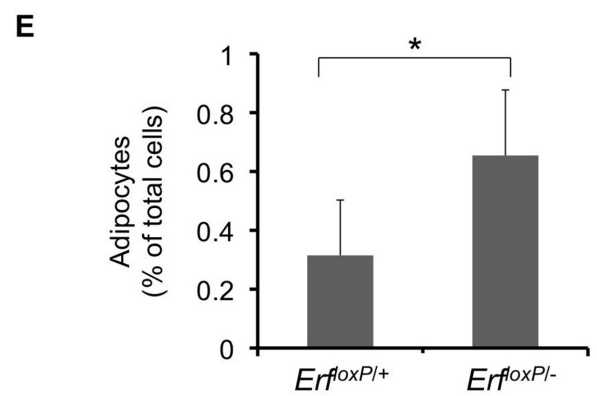
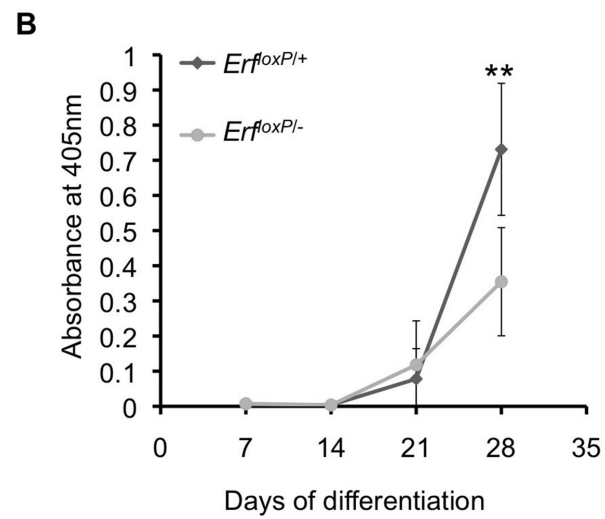
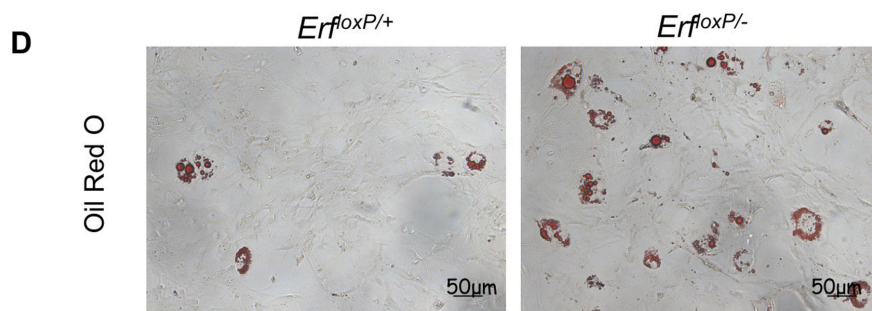
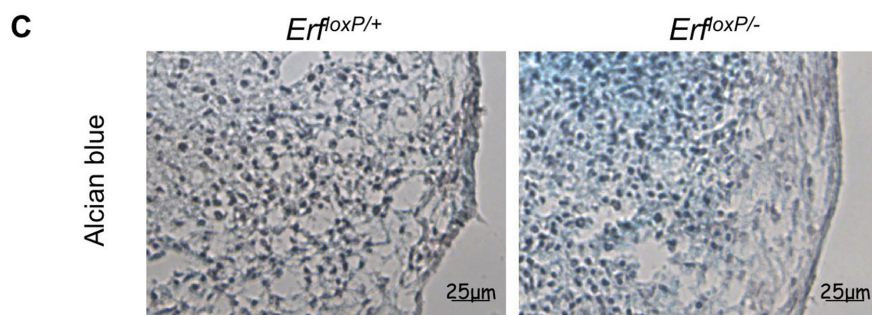
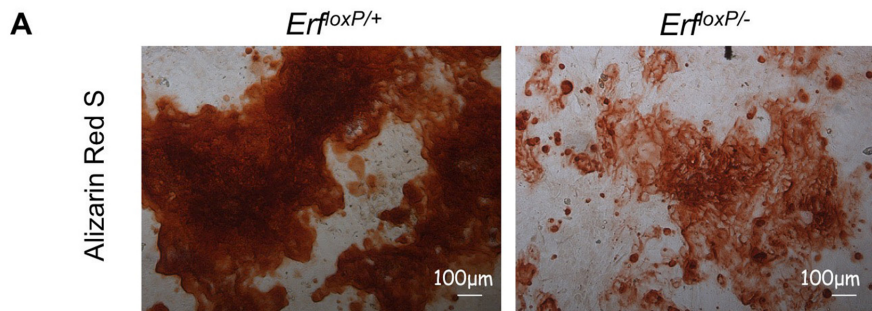
904

905



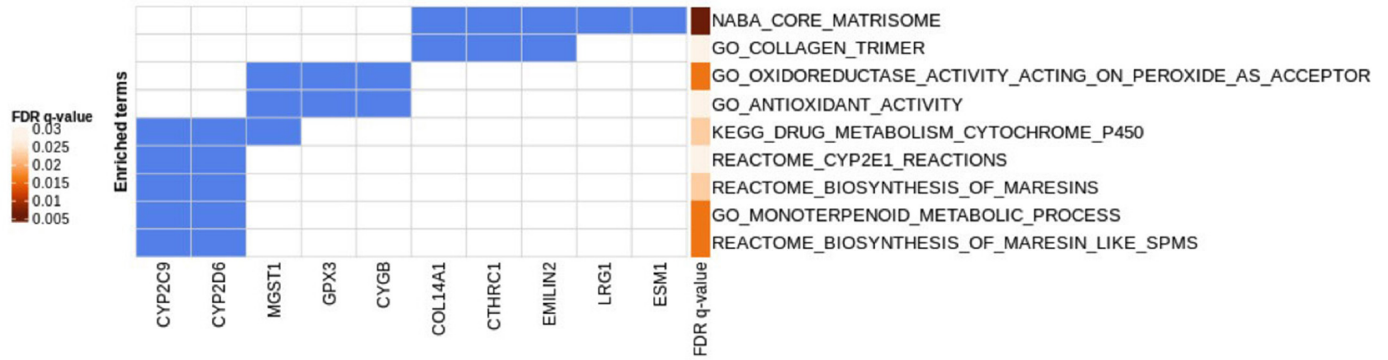




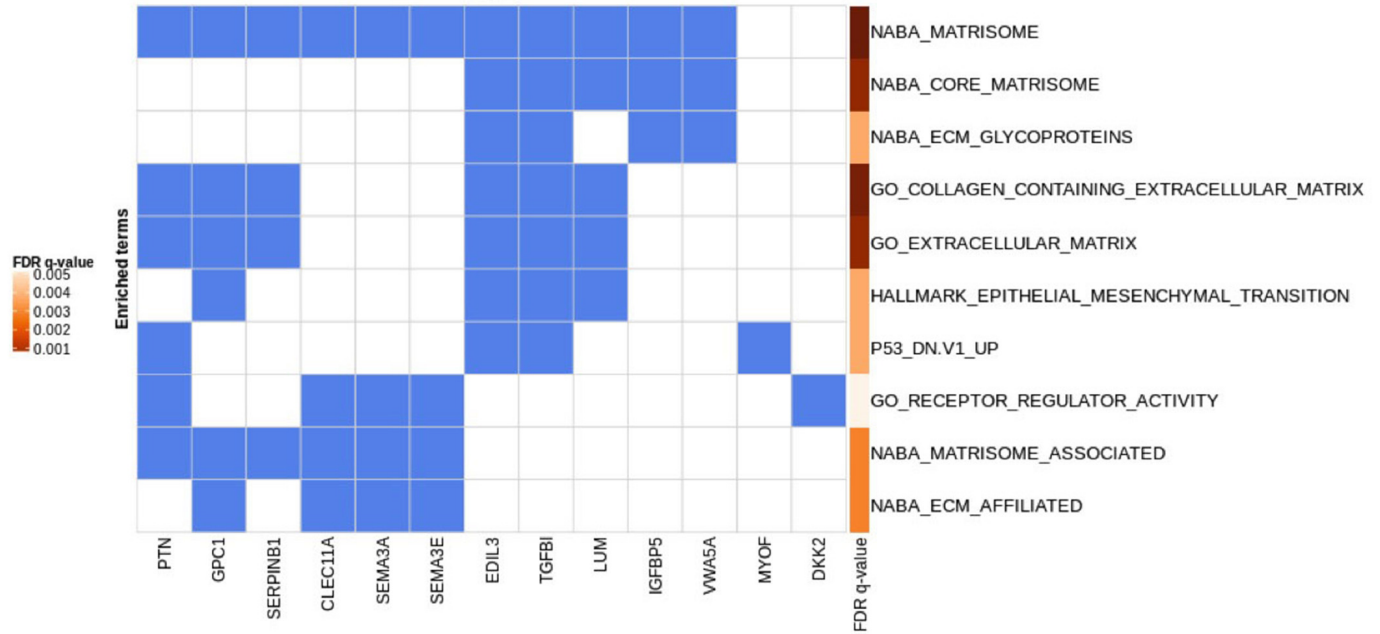




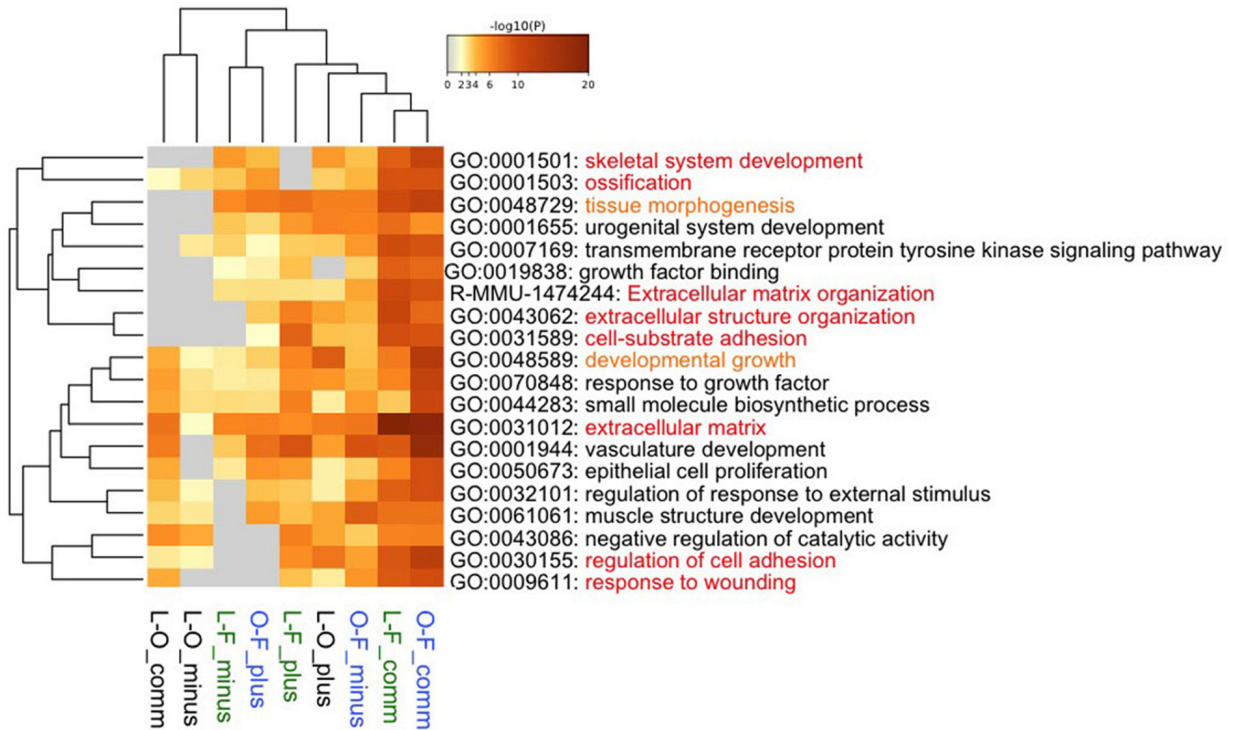
A



B

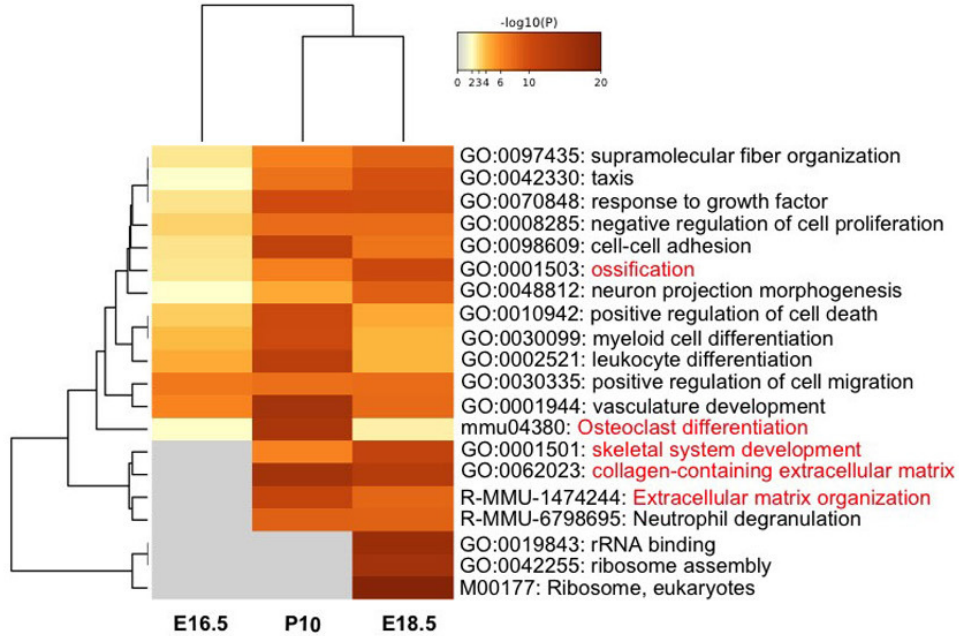


C

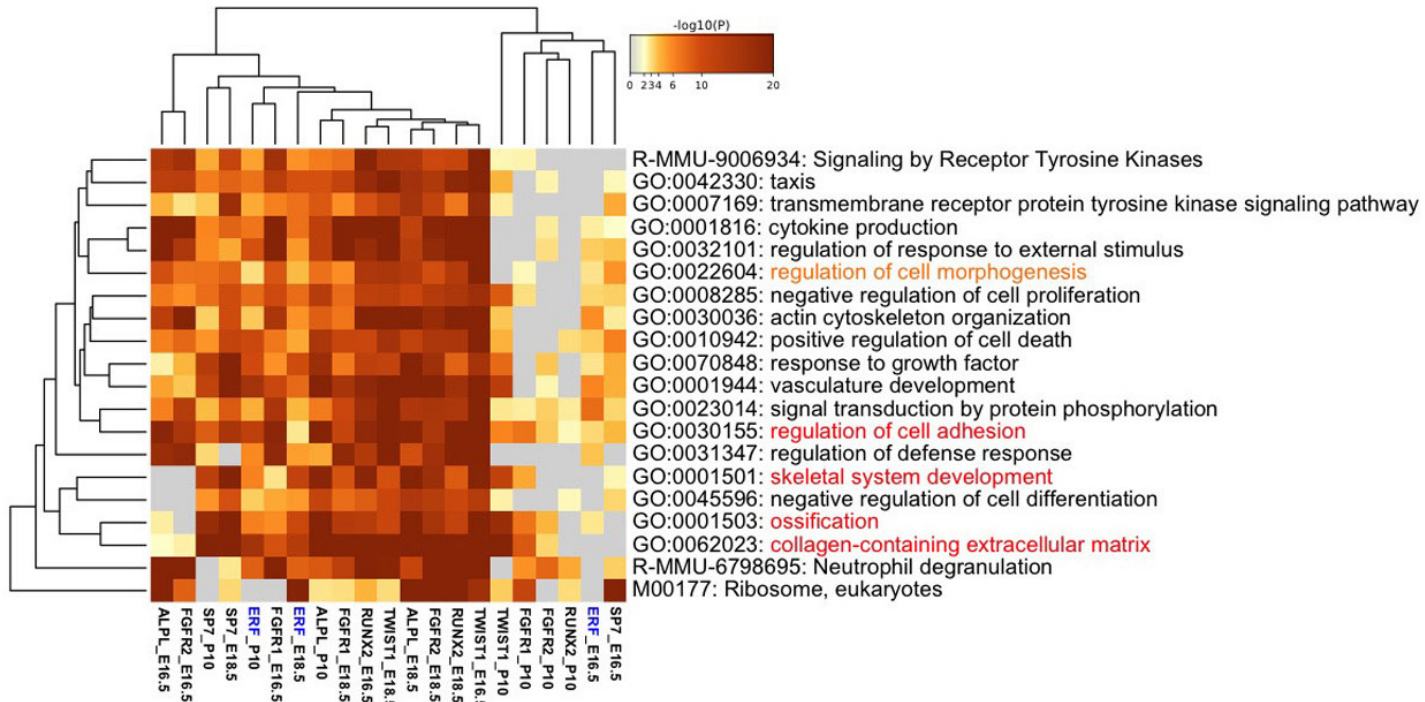


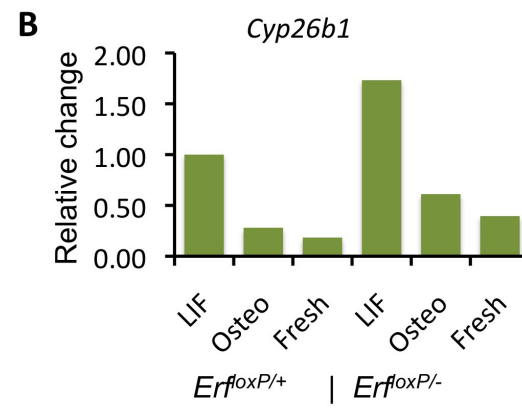
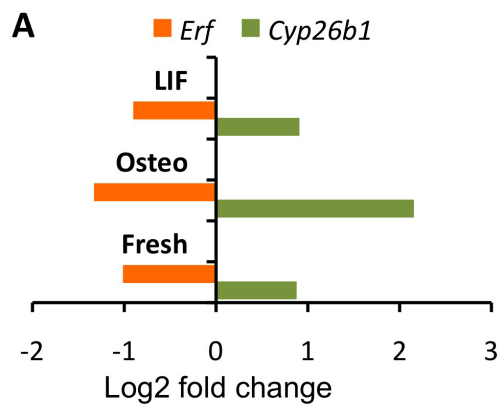


A



B





**C**

Different in:	<i>Erf<sup>loxP/+</sup></i> and <i>Erf<sup>loxP/-</sup></i>	<i>Erf<sup>loxP/+</sup></i> -only	<i>Erf<sup>loxP/-</sup></i> -only
pValue	1.67 10 <sup>-8</sup>	1.06 10 <sup>-8</sup>	0.002
qValue	1.02 10 <sup>-7</sup>	7.00 10 <sup>-8</sup>	0.003
Bonferroni	2.76 10 <sup>-6</sup>	1.75 10 <sup>-6</sup>	0.287

